CIRP Journal of Manufacturing Science and Technology 35 (2021) 659–674

Contents lists available at ScienceDirect

CIRP Journal of Manufacturing Science and Technology

journal homepage: www.elsevier.com/locate/cirpj

Full-length article

High-pressure flank cooling and chip morphology in turning Alloy 718

Nageswaran Tamil Alagan[a,*], Pavel Zeman[b], Vladimir Mara[c], Tomas Beno[a], Anders Wretland[d]

[a] Department of Engineering Science, University West, Trollhättan, Sweden
[b] Department of Production Machines and Equipment (RCMT), Faculty of Mechanical Engineering, Czech Technical University in Prague, Czech Republic
[c] Department of Material Engineering, Faculty of Mechanical Engineering, Czech Technical University in Prague, Czech Republic
[d] GKN Aerospace Engine Systems AB, Trollhattan, Sweden

ARTICLE INFO

Article history:
Available online xxx

Keywords:
Alloy 718
Chip segmentation
Chip morphology
Flank cooling
Chip contact area
Round insert
Tungsten carbide

ABSTRACT

The use of cutting fluids is commonly considered a necessity while machining Heat Resistant Super Alloys (HRSA). Specifically, cutting fluids applied under high-pressure, which for many decades have been the solution for the most demanding applications. The results might be diverse and vary between applications, but typically leads to improved tool life, enhanced chip breakability, lower temperature in the cutting zone and better surface quality of the finished product. The available high-pressure cutting fluid delivery systems are usually designed with the intention to improve the cutting fluid penetration at the vicinity of the cutting edge on the rake face side of the insert. However, there has been limited interest in investigating high-pressure cutting fluid applied to its flank face. Both specifically and in combination with cutting fluid directed to the rake face. In this study, the focus has been to investigate the chip formation process during the turning of Alloy 718 (Inconel 718). Particularly, for a defined turning operation where high-pressure cutting fluid is applied to the flank side as well as the rake side of an uncoated carbide insert. Several combinations of pressure levels and jet directions were investigated. The corresponding effects on the tool-chip contact zone and chip characteristics were studied for two cutting speeds. The results of the investigation showed a substantial improvement in lowering the tool-chip contact area at a rake pressure of 16 MPa. At which pressure, additional cutting fluid applied to the flank at a moderate pressure of 8 MPa had no dominant effect on chip formation (chip break). However, flank cooling of the cutting zone supports chip segmentation and thus indirectly chip breakability. For cutting fluid applied to the rake side at a more moderate pressure of 8 MPa, more prominent effects on the insert became apparent when additional cutting fluid was applied to the flank side. This was particularly noticeable when cutting fluid was directed towards the flank side of the insert at the same pressure level as the cutting fluid applied towards its rake face. The additional thermal transfer was seen to have a significant effect on the material deformation phenomena in the primary shear zone (lowering shear angle) as well as the sliding and sticking conditions of the tool-chip interface.

Based on the evidence from this study, it can be concluded that cutting fluid applied towards the flank side of the insert has a significant impact on the cutting process. In particular, if applied in combination with a rake pressure at a similar level, in this case, 8 MPa.

Introduction

The technological advancement in and around the metal cutting industry has incremented towards better understanding and optimization of its processes. One such increment is improved tool utilization, which ultimately helps driving manufacturing and production of different materials towards improved sustainability and a reduced environmental footprint. However literary a vast number of new advanced materials are added to the catalogue of *difficult to machine* alloys in the meantime. Heat Resistant Super Alloys (HRSA) are among those where there still exists a clear incentive to find and apply manufacturing concepts that distinguish them from the currently available. A challenge that is constantly encountered.

HRSA have found their natural place on the material shelf of aerospace industries due to their mechanical and physical properties. Components manufactured from high-performance materials like these are widely used in the turbine's hot sections. Specifically, for their ability to retain mechanical and physical

* Corresponding author at: Department of Engineering Science, University West, Gustava Melins Gata 2, 461 32 Trollhattan, Sweden.
E-mail address: nageswaran.tamil@hv.se (N. Tamil Alagan).

https://doi.org/10.1016/j.cirpj.2021.08.012

properties such as creep and corrosion resistance at elevated temperatures. One HRSA in particular, the Alloy 718, acts as a base material to manufacture components used in such demanding applications. However, despite its long and widespread use, it is still a challenge to machine Alloy 718 at high levels of productivity.

In the following, the results of an extensive investigation of the intrinsic properties of the removed material (the chips) while using cutting fluid applied on both the rake and the flank side of the cutting edge are presented.

In the primary part of the research work – [1] – tool wear and friction mechanisms during machining are in focus and in particular, the effects from high-pressure cooling applied to the flank side of the insert.

In the secondary part – the present report – the tool-chip contact area and obtained chip morphology is investigated Fig. 1(a).

The layout of the investigation approach is illustrated in Fig. 1(b).

Thus, the machining strategies used for this investigation, media application concepts and equipment such as tool holders (high-pressure) and machine tools are all same and described in Ref. [1].

Many researchers have previously reported the advantages of high-pressure coolant assisted machining, particularly while turning nickel-based alloys. Among the reported benefits were improved chip break capacity, less tool wear and reduced tool-chip contact length as depicted e.g. by Klocke et al. [2]. On the other hand, higher cutting forces were observed with increasing cutting fluid pressure as compared to conventional cooling. However, all the reported effects correlate with a significant drop of the temperature in the cutting zone with increased cutting fluid pressure and flow rate. The applied cutting fluid transfers heat from the deformation zone and suppresses the temperature there, as described by Armarego and Brown [3]. Thus, the strength of the material while moving through the deformation zone is retained at a higher level as compared to conventional cutting fluid application. Hence, higher shear work for chip formation is necessary. Subsequently, the chip is more brittle and better breakable.

Further, high-pressure application of cutting fluid creates a hydrodynamic wedge and lifting the chip off the rake face as described by Sharman et al. [4]. Thus, the chip curvature is higher, and the tool-chip contact can be reduced. These conditions and higher cutting forces are changing the stress distribution on the rake face — the ratio between the length of the sticking and sliding zones. As Machado and Wallbank claimed [5], the mechanical action of the pressurized cutting fluid significantly reduces the sliding zone between the tool and chip. On the other hand, the sticking zone is affected marginally. A higher value of the ratio sticking/sliding regions decreases the value of the coefficient of friction as explained in Armarego and Brown [3]. Thus, the friction exerted in the tool-chip interface can be reduced with high-pressure cooling.

An increase of cutting fluid pressure did not influence surface integrity much, according to Sharman et al. [4]. Cooling of the flank can reduce tool wear and friction between the tool and machined surface. Moreover, it was pointed out that higher temperature at low cutting fluid pressure causes steam barrier owing to vaporization of fluid and therefore prohibits the fluid from efficiently penetrating the cutting zone. Similar effects of high-pressure cutting fluid applied to the rake face were described in Ahmed et al. [6]. Although it was validated for stainless steel, the phenomena are similar. Pressurized cutting fluid creates a wedge. Subsequently, chips are more curved and shorter. Cutting fluid penetration into the tool-chip interface reduces temperature and friction.

An important factor in high-pressure cooling is the combination of applied pressure and flow rate. This should be optimized for maximum heat dissipation from the cutting zone, as reported by Dahlman [7]. A high flow rate and high-pressure combined gives the cutting fluid capacity to extract more heat from the cutting zone due to the extra deep penetration achieved by the maximized impact (force) from the coolant jet. Further, their temperature measurement results showed a significant reduction in temperature and flank wear land [8].

The impact of high-pressure cutting fluid on chip formation has been investigated in detail in different aspects by several researchers. An overview of the necessity of chip control as an important aspect of machinability was published in 1993 by Jawahir and Luttervelt [9]. They investigated chip breakability, influences of cutting fluid/lubricant, modelling and cutting conditions. They also reported that using a coolant increases the chip curl and lowered the tool-chip contact area. That is according to the theory explained above. However, the effect of higher pressure as well as cooling of the flank were not extensively discussed in the study.

In the 1990s Machado and Wallbank [5] were one of the first to investigate and present an overview on enhanced chip control by increased cutting fluid pressure applied to the rake face. Their study aimed for various cutting conditions when turning the Ni-base superalloy Inconel 901. They brought evidence of a reduction

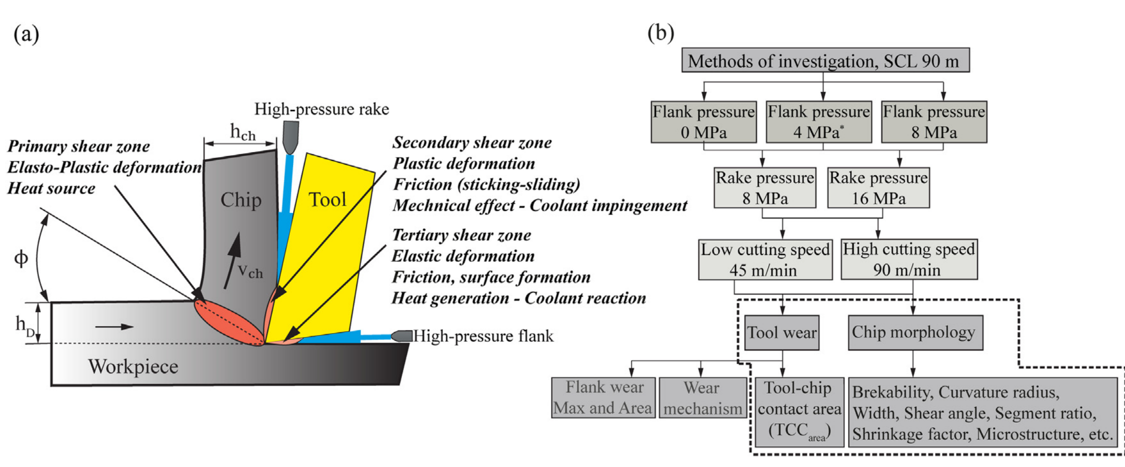

Fig. 1. (a) Illustrates and describes the three shear zones with a focus on high-pressure cutting fluid application; (b) Overview of the research methodology, incorporating investigation methods and process conditions focussed on TCC_{area} and Chip morphology adapted and reconstructed from Ref. [1].

in the tool-chip interface temperature by means of measured higher cutting forces. They also demonstrated that the more curved, segmented, and smaller chips are all effects of cutting fluid applied under high-pressure. Nevertheless, no detailed analysis of the chip formation (chip thickness, chip curvature, tool-chip contact length, etc.) was presented for an explanation of the observed phenomena.

Ezugwu and Bonney [10] investigated the benefits of high-pressure coolant applications with respect to chip breakability, tool wear and cutting forces. Their investigation was focused on turning Alloy 718 with coated cemented carbide tools. The results confirmed the ability of the cutting fluid to lift the chip and reach closer to the cutting interface. Thus, lowering the friction coefficient and in turn, reduce the temperature in the sliding zone. It is argued that consequently, also forces are reduced. On the other hand, decreased forces are in contradiction to Klocke et al. [2] and Machado and Wallbank [5]. It is further reported that improved chip segmentation is achieved at a rake pressure of 20.3 MPa, while 15 MPa had only a negligible effect on chip breakability. However, a detailed inspection of the chip formation in support of the described observations was not undertaken.

When assessing the investigations of Machado and Wallbank [5] and Ezugwu and Bonney [10], it is clear that their results illustrate that cutting fluid pressure is not the only factor that affects chip control. The overall cutting conditions and the type of cutting tool used plays critical roles in an optimized set-up. Also, when cutting fluid is applied at high-pressure.

Furthermore, Çolak [11] pushed the high-pressure of rake cutting fluid up to 30 MPa in turning Alloy 718 by coated carbide tools. The results are well aligned with the findings of Ezugwu and Bonney [10]. Considerably lower cutting forces were indicated with high-pressure cooling. It was shown that an increase in pressure lowered the tool-chip contact area and chip curvature radius. The theory for better chip breakability at higher application pressures as compared to flood cooling was proved again. Moreover, the author showed that chip breakability was significantly influenced by the feed rate and depth of cut. Nevertheless, no detailed study of chip morphology related to process parameters and material properties are presented for validation of the theory behind this phenomenon.

Crafoord et al. [12] were one of the few researchers in the 1990s to conduct extended investigations in studying the application of media under high-pressure solely focussed on chip control. The relation between pressure (16–77.2 MPa), nozzle diameter, flow rate, cutting fluid pressure and jet velocity and their impact on chip up-curl radius was investigated. Findings showed that the chip radius was found to be primarily proportional to the applied jet power.

Öjmertz and Oskarson [13] further increased the applied pressure with a specific water-jet system up to 360 MPa and studied its influence in turning Alloy 718 with ceramic cutting tools. They fully confirmed a hydro-wedge effect of the applied high-pressure cutting fluid behaves like a mechanical chip breaker on the cutting tool. At such high pressures, the cutting fluid could penetrate and access the very proximity of the cutting edge, which led to small chips. This may affect friction in both the sliding and the sticking region. A decrease in the total chip length and thickness was observed with increasing pressure even though thicker segments were created. However, the chip length and compression ratio did not change significantly for pressures higher than 100 MPa. Unfortunately, no detailed clarification for this behaviour was done.

Khan et al. [14] studied the chip shape when turning a titanium alloy with the rake and flank coolant at 8 MPa. A combination of both coolants lowered the main cutting force and reduced the cutting temperatures for the entire range of cutting conditions in comparison to dry turning. This correlates with the results reported by some of the previously mentioned research work. The chips were thicker with high-pressure cooling but this is in contradiction to Öjmertz and Oskarson [13]. However, the chips became thinner with increased cutting speed as an increased shear angle can be expected. The authors mentioned that a rake pressure of 8 MPa is too low for significant changes in chip segmentation. Despite the fact that the coolant affects both the friction between the tool and the chip as well as the contact length. This was confirmed by lower cutting temperature, lower cutting forces and a higher chip reduction coefficient for the case of high-pressure coolant application as compared to conventional coolant application. Although flank cooling was applied, it was not possible to separate and describe the effects of chip formation.

Thus, state-of-the-art, extracted from the contributions of the listed researchers show that the main focus has been directed towards the tool rake and the influence of directed high-pressure media jets towards the tool-chip interface and only, a very scant focus was aimed for the study of effects on the chips from high-pressure media applied to the flank [1].

Some of the previous research work also illustrated the requirement to have extra high-pressure (more than 20 MPa) to achieve the sought for chip break effects. Thus, there still exists a research interest in whether it can be possible to substitute extra high-pressure rake cooling demands by flank cooling. Especially, since systems for media application while using extra high-pressures are complicated, have large energy demands and high costs. Not to mention operator safety and environmental complexity. Further, before this study, there was no investigation conducted with a clear aim for the effects on the chip by combining both rake and flank pressure cooling. In addition, only limited research has been conducted on the use of round cutting inserts and their influence on chip morphology.

From this, it is explicit that there exists a knowledge gap in the combination of high-pressure media applied to the third shear zone i.e., the tertiary shear zone (flank face) while cutting Alloy 718 with a round insert. In particular with respect to the obtained chip morphology.

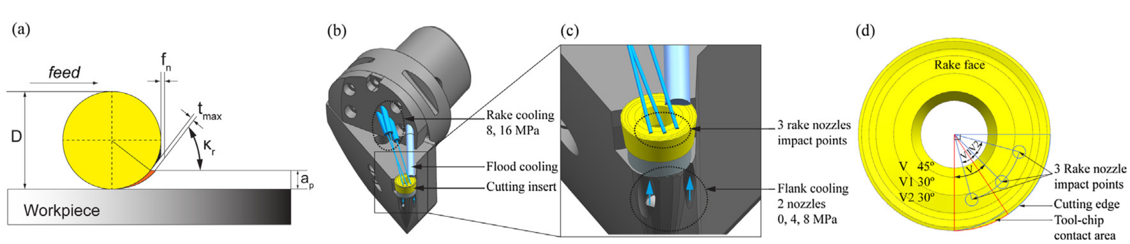

Fig. 2. (a) Illustration of the contact between a round insert and a workpiece producing varying chip thickness up to the maximum; (b) Tool holder CAD model with internal delivering to rake and flank faces; (c) Magnified view to the cutting tool and impact directions; and (d) Cutting fluid impact points on the rake face extracted from Ref. [1].
Remark:
For the flank pressure condition of 4 MPa, only its effect on TCC_{area} was investigated.

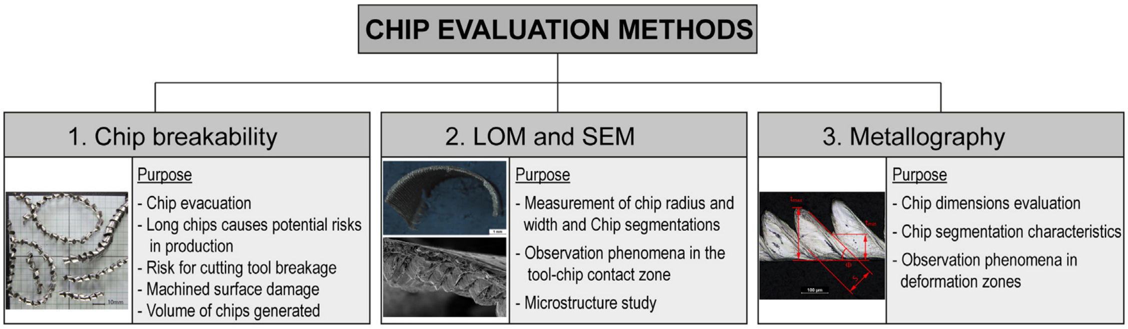

Fig. 3. Chip investigation methodology.

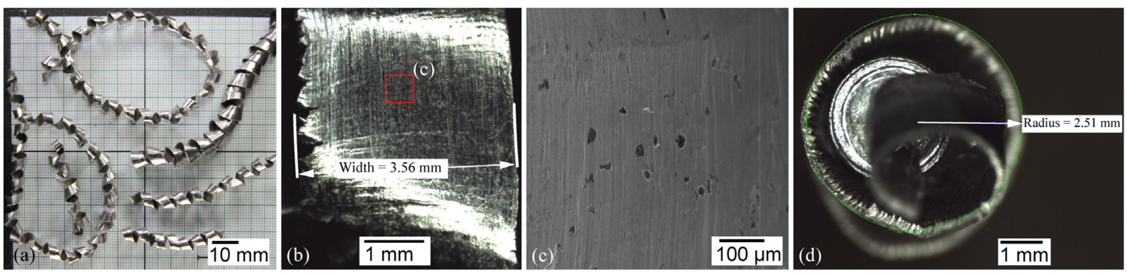

Fig. 4. Evaluation of the chip: (a) general shape (b) width, (c) SEM micrograph of selected area and (d) curvature radius.
Remark:
All the chips were scanned for higher detail by SEM with a secondary electron detector for both chip edge side and tool interface side views. In addition, for one set of results (chips), a stereomicroscope (*Nikon SMZ 1500*) was used to capture the *general view* of the chip, see Fig. 11.

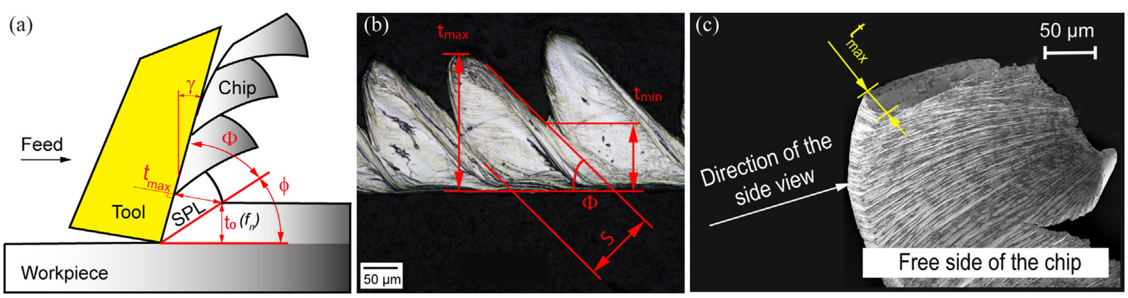

Fig. 5. (a) Description of parameters in the chip formation process, SE micrograph; (b) Metallography chip sample-illustrating thicknesses and shear angle; (c) Chip image illustrating the side view and t_{max}.

The present investigation aims to close that gap and research the benefits of high-pressure flank cooling (up to 8 MPa), in combination with rake pressure (up to 16 MPa). The arrangements and experimental set-up is based on previous work by the authors [1] in which the focus was tool life and wear mechanisms, but did not include a thorough chip study. The experimental out-set of the present investigation is based on the same cutting and cutting fluid conditions [1].

Terminology and nomenclature

Symbol	Abbreviation	Unit
HRSA	Heat Resistant Super Alloys	
LOM	Light Optical Microscopy	
SEM	Scanning electron microscopy	
SE	Secondary electron detector	
SCL	Spiral cutting length	m
f_n	Feed per revolution	mm/rev
a_p	Depth of cut (DOC)	mm
MR	Material removed	cm^3
v_c	Cutting speed	m/min
RP	Rake pressure	MPa
FP	Flank pressure	MPa
v_{ch}	Chip speed	m/min
TCCarea	Tool Chip Contact area	mm^2
©$_o$	Rake angle	°
Φ	Angle of segment orientation	°
φ	Shear angle	°
t_{max}	Maximum chip thickness	mm
t_{min}	Minimum chip thickness	mm
t_0	Undeformed chip thickness	mm
t_c	Equivalent chip thickness	–
S	Segment width	mm
G_s	Segment ratio	–
ζ	Shrinkage factor	–
b_{ch}	Chip width	mm
r_{ch}	Chip curvature radius	mm

Experimental set-up and procedure

Details of the setup

The hydraulic setup is chosen such that it corresponds to the first part of this investigation, as reported in Ref. [1]. The major reason for the application of cutting fluid at high pressure is to

Table 1
Measurement results of tool-chip contact area with standard deviation.

S.no	v_c (m/min)	Rake pressure (MPa)	Flank pressure (MPa)	$TCC_{area} \pm SD$ (mm^2)
1	45	8	0	0.91 ± 0.10
2	45	8	4	0.91 ± 0.09
3	45	8	8	0.74 ± 0.06
4	45	16	0	0.70 ± 0.08
5	45	16	4	0.65 ± 0.10
6	45	16	8	0.60 ± 0.07
7	90	8	0	0.90 ± 0.08
8	90	8	4	0.95 ± 0.03
9	90	8	8	0.88 ± 0.01
10	90	16	0	0.78 ± 0.03
11	90	16	4	0.76 ± 0.06
12	90	16	8	0.76 ± 0.06

improve its reachability such that the cutting fluid will maintain its thermal properties when and while in contact with the members of the cutting zone (chip, tool, workpiece). Thus, the hydraulic conditions with respect to heat transfer must at least be balanced such that the heat generated from the cutting process is on par with the conditions of the cutting fluid applied under high pressure. This implies that the pressure of the cutting fluid at the impact area must be - ideally - larger than the pressure corresponding to the *Leidenfrost temperature* [15].

The second vital, but equally important quality, is to create a mechanical force at the rake face to reduce the tool-chip contact area and to attain an effective chip breakability. This is reached through the combination of speed and flow rate of the cutting fluid which is in relation to the following governing equations of mass flow (1) and energy conservation (2) correspondingly [12]:

$$\dot{m} = \rho \cdot v \cdot a \tag{1}$$

$$v = 2\sqrt{p} \tag{2}$$

$\dot{m}$ – mass flow rate; ρ – density; v – jet speed; a – area; p – pressure

The machining setup is based on a 5-axis vertical CNC turning centre was used for face turning a cast Alloy 718 ring (average hardness of 381 ± 21.8 HV). The detailed machine setup can be seen in Ref. [16]. The machine tool was programmed to increase the spindle speed as the cutting tool moved towards the table (spindle) centre to achieve constant cutting speed. The outer diameter of the ring was 742 mm, and the inner diameter was 672 mm. The machined length, l_m, of approx. 8 mm. The spiral cutting (SCL) of 90 m, feed of 0.2 mm/rev, depth of cut (DOC) of 1 mm and material removed (MR) of 18 cm^3 was kept constant.

A water-based emulsion with a concentration of 5% (petroleum-based additive mixed with water) was used as a cutting fluid at room temperature. The cutting fluid was supplied at high pressure to both the rake face (three nozzles each with a diameter of 0.8 mm) and the flank face (two nozzles, each of diameter 1.2 mm) through a specially designed tool holder. Three flank pressures of 0, 4 and 8 MPa for two rake pressures 8 and 16 MPa at a cutting speed of 45 (low) and 90 (high) m/min with a corresponding cutting time of 2 and 1 min describes the experiment in short.

Each experimental condition was repeated two times, to ensure adequate repeatability. The tests were randomized before experimenting. Further detailed descriptions can be found in the experimental section of Ref. [1].

Round uncoated cemented carbide inserts with the ISO designation RCMX 12 04 00 (edge has a negative facet on rake face: γ_o = −17 °, in the tool orthogonal plane) and grade of H13A were used as cutting tools. The WC tools are commercially available and cost-effective. In rough machining of HRSA, round inserts are widely used due to their maximum edge strength and extended usage of the cutting edges by clever indexing. Nomenclature as well as the specification of the insert edge geometry is described in Ref. [16]. The engagement/position of the cutting tool in relation to the workpiece during machining is illustrated in Fig. 2. It is to be noted that round inserts have not been subject to extensive use in previous research and its shape in itself complicates the chip study. The round cutting edge presents a particular challenge in that it produces a variable un-deformed chip thickness along the cutting edge from zero to maximum (t_{max}).

Remark:

For the flank pressure condition of 4 MPa, only its effect on TCC_{area} was investigated.

Investigation methodology

The procedure to measure the TCC_{area} was based on a contact angle of 34 ° on the rake face (a detailed explanation can be found in Ref. [17]) and a 3-D scanning microscope. Different aspects of the chip morphology were evaluated as shown in Fig. 3.

Measurement of chips

The chip shape was captured by a digital camera equipped with a macroscopic lens see Fig. 4(a). Further width and curvature radius were measured by light optical microscope (LOM), Fig. 4(b & d). Ten chips for each condition (chips were selected which looked more uniform to each other) were measured for robustness of the results. In Fig. 4(c) scanning electron microscope, SEM (*JEOL JSM 5410*) using secondary electron (SE) detector shows high magnification of the selected area of the chip surface (tool side) see Fig. 4(b).

Remark

All the chips were scanned for higher detail by SEM with a secondary electron detector for both chip edge side and tool interface side views. In addition, for one set of results (chips), a stereomicroscope (*Nikon SMZ 1500*) was used to capture the *general view* of the chip, see Fig. 11.

Metallography sample preparations of chips

After the physical measurements of the chips such as thickness, width, radius, selected chips were prepared. These represent the following test conditions: two rake pressures (8 and 16 MPa), two flank pressures (0 and 8 MPa) for both cutting speeds and were prepared for the metallography investigations.

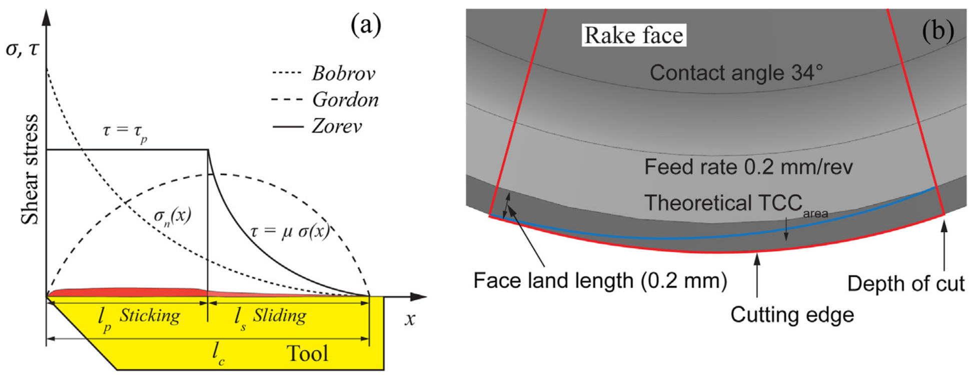

Fig. 6. (a) Shear stress distribution adapted and reconstructed from Refs. [23,24,27]; (b) CAD illustration of theoretical chip contact area for feed rate 0.2 mm.

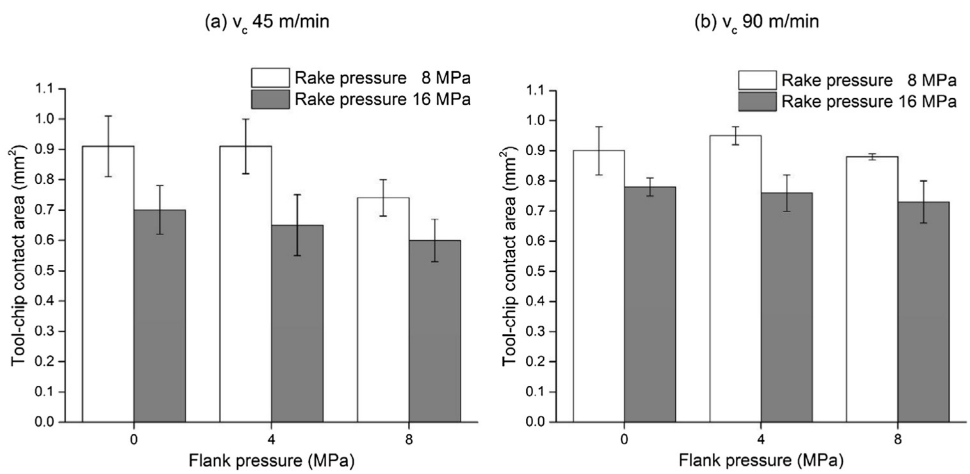

Fig. 7. Comparison tool-chip contact area for different cutting speeds, rake and flank pressures.

The measurement procedure described step-by-step:

- The chip was pressed in STRUERS Multifast Phenolic Hot Mounting Resin.
- A P1000 sandpaper was used for rough grinding.
- Pre polishing: Canvas and diamond suspension BUEHLER METADI 3 μm.
- Final polishing: Canvas and Al_2O_3 BUEHLER MASTERPREP Polishing Suspension 0.05 μm.
- Samples were etched by STRUERS Polipower source in a solution of 10% oxalic acid for 8 s.

Lastly, the metallography pictures of all chips were taken by an optical microscope (*Carl Zeiss Neophot 32 with a digital camera*) and the analytic software *Nis Elements AR* was used to measure the chip segmentation parameters.

Measurements and calculations from metallography chip samples

The methods and principles of evaluation were set based on the previous researcher's findings/observations Refs. [18–21]. The chips were prepared as metallographic samples to describe more precisely the changes in primary and secondary shear zones with cutting fluid for both cutting speeds. These parameters were the angle of segment orientation (Φ), shear angle (ϕ), maximum chip thickness (t_{max}), minimum chip thickness (t_{min}), equivalent chip thickness (t_c), segment width (S), segment ratio (G_s) and shrinkage factor (ζ). Some of these parameters can be seen in Fig. 5. The rest of them are calculated from Eqs. (3) to (6). In general, three chips for every condition were inspected. All the mentioned parameters were evaluated for ten segments of each chip. A marked single segment can be seen in Fig. 5(b).

$$t_c = t_{min} + \frac{t_{max} - t_{min}}{2} \quad (3)$$

$$G_s = \frac{t_{max} - t_{min}}{t_{max}} \quad (4)$$

$$\phi = \arcsin\left(\frac{t_0}{t_{max}} \cdot sin\ \text{F}\right) \quad (5)$$

$$\zeta = \frac{\sin\phi}{\cos(\phi - \gamma)} \quad (6)$$

Results and analysis

The investigation is aiming for an enhanced understanding of the influence of high-pressure cutting fluid directed towards the rake side as well as the flank side of an insert (the cutting edge in general terms), and more precisely. How variations in the applied cutting fluid pressure correlate with the attained Tool Chip Contact-area (TCC_{area}).

Table 2
The overview of chip parameters and their theoretical explanation.

Symbol	Abbreviation	Reason for evaluation and current knowledge
Φ	Angle of segment orientation	The parameter is necessary for calculating the shear plane angle. The angle decreases as the v_c and f_n increases.
φ	Shear angle	An important factor that describes the chip formation process. Theoretically, it increases significantly with v_c (higher localisation of plastic deformation in the primary shear zone) and f_n (increases the un-deformed chip thickness).
t_c	Equivalent chip thickness	Describes chip thickness more precisely when segmented/serrated chip is generated. In general, it increases with the f_n and decreases with v_c.
S	Segment width	Depicts the structure of the chip in detail. It is an additional evaluation parameter to the chip thicknesses. Bigger segments are generated when the un-deformed chip thickness increases [18]. The parameter also increases as the localisation of plastic deformation in the primary zone increases. This leads to the transformation of a continuous chip into segmented.
G_s	Segment ratio	Defines the level of chip segmented, a higher value indicates that chip and individual segments are less cohesive to each other owing to the lower contact area between the chip segments. Therefore, chip breakability improves at higher G_s. In general, this ratio increases with the v_c.
ζ	Shrinkage factor	Theoretically, it is lower than the value of 1, an increase in v_c causes the factor to increase because a thinner chip is generated. Although no significant influence of v_c and f_n can be observed [18,19].
b_{ch}	Chip width	An important factor for the description of the chip deformation in the direction along the cutting edge. Theoretically, the width is a constant with the change of v_c and f_n.
r_{ch}	Chip curvature radius	Describes strain in the chip and its total deformation, it decreases as the rake pressure increases [20]. A smaller radius means the chip can break more easily into shorter elements. The radius increases with the depth of cut and with cutting speed.

The results are explained in the following sections.

Tool-chip contact investigation

High-pressure cutting fluid is extensively used with the main purpose to improve tool life. This is primarily achieved by lowering the temperature in the cutting zone, but also by boosting the mechanical effects of breaking the chips generated at the rake side of the tool. Thus, reducing coherent friction effects in the zones where sliding occurs between the tool and work material. In this study, the response from the applied hydrodynamic forces is primarily detected by measuring the Tool Chip Contact-area (TCC_{area}). The TCC_{area} is derived from measurements by use of a 3-D scanning microscope and tabulated in Table 1.

The primary justification for the application of cutting fluid at high pressure to the material removal process is to improve the reachability of the cutting fluid for effective heat transfer from the cutting zone [2,22]. The second vital and important quality is to create a mechanical force at the rake face to reduce the tool-chip contact area and to attain an effective chip break capacity. Consequently, the friction between the tool and chip is reduced which eventually leads to lower tool wear.

Both compressive and shear stresses act on the Tool Chip Contact area (TCC_{area}). The workpiece material undergoes plastic deformation while the material passes through the primary shear zone during which the temperature is significantly elevated. The chip is forced to move along the rake face where further deformation occurs in the secondary shear zone. More heat is generated of which some is transferred to the cutting tool [23,24].

Similarly, the flank section of the cutting edge is influenced by variations in contact pressure from the workpiece, which in combination with the prevailing friction conditions and relative speed will lead to an added thermal load on the cutting edge. Thus, the cutting edge is exposed from heat generated at its rake side as well as its flank side. The variation in temperature levels in these areas (rake: chip; flank: workpiece) will create a temperature field in the direction towards the volume of the tool that exhibits a lower temperature. Presumably, towards the inner parts of the cutting edge, but also towards the sliding interface between the workpiece material and the flank of the insert. Arguably, under the assumption that the new surface just generated on the work material exhibits a lower temperature than that of the corresponding material volume of the tool, despite the temperature rise from the just undergone deformation [2,25,26].

Through the exposure of the flank face of the cutting edge (and simultaneously the workpiece) to forced cooling, the mentioned temperature field can be controlled. Thus, variation of the cutting fluid pressures applied to the flank face for the two pressure conditions applied to the rake face is expected to improve the thermal exchange in the cutting zone and consequently affect the chip formation through the concurrent change in friction at the rake face of the tool [22,26].

To evaluate the influence of *flank cutting fluid* in relation to *rake cutting fluid*, the tool-chip contact area is measured for all the investigated cutting conditions and tabulated in Table 1 (including their deviation expressed as $\pm$ SD). The tool-contact length was not measured due to the varying chip thickness along the cutting edge as shown in Fig. 6(b). However, the theoretical maximum contact length of 0.2 mm is expected to be at the depth of cut.

A comparison of the shear stress distribution proposed by *Bobrov*, *Gordon and Zorev* is shown in Fig. 6(a).

Bobrov and Gordon did not suggest any distinction in the tool-chip contact. However, according to *Zorev's* model, the rake face, total tool-chip contact length, l_c, comprises of two zones.

- The first zone is sticking, (l_p), see Fig. 6(a), or seizure, near the cutting edge, where the chip is deformed in shear by high frictional stress. In the sticky zone, the tangential load is equal to the yield strength of the material. Seizure is defined as a solid phase weld between the primary atomic bonds of clean metallic surfaces.
- The second zone is sliding (l_s), where interfacial sliding occurs due to the relative motion between the outermost layer of chip material (atoms, grains) and rake face. In this zone, the friction coefficient is constant and equal to the coefficient of friction between the workpiece and tool material. The state of the sliding zone depends on the cutting conditions as well as the properties (mechanical and thermal) of the interacting materials (tool and workpiece) [23,24,27,28].

The high-pressure cutting fluid jets (mechanical force) directed towards the rake face are expected to be able to penetrate close to the proximity of the cutting edge. Thus, impacting the chip interface leading to reduce the sliding region and contact area on the rake face. Further elevated media pressure on the flank side in combination with the applied cutting fluid jets on the rake side will provide for maximum heat dissipation [1,2,22].

Consequently, the TCC_{area}, as the expected response to be influenced by the overall temperature in the cutting zone, is

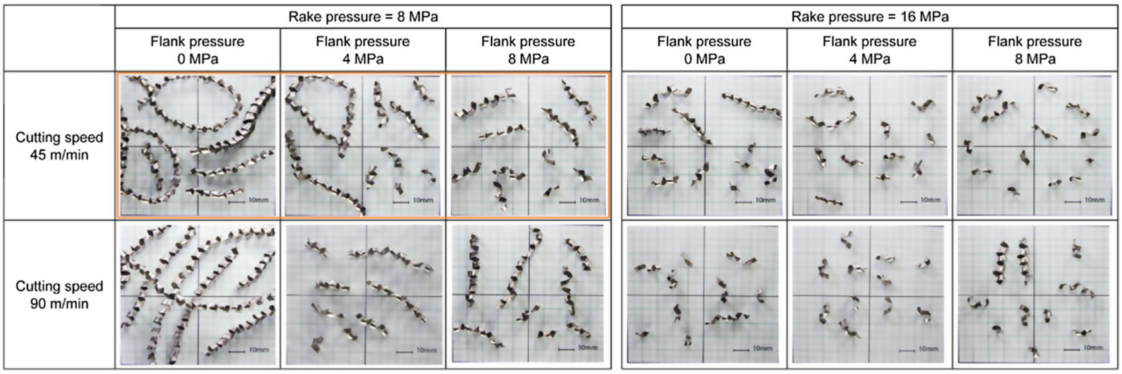

Fig. 8. Comparison of shape and length of the chip for varying conditions of rake pressures, flank pressures and cutting speeds.

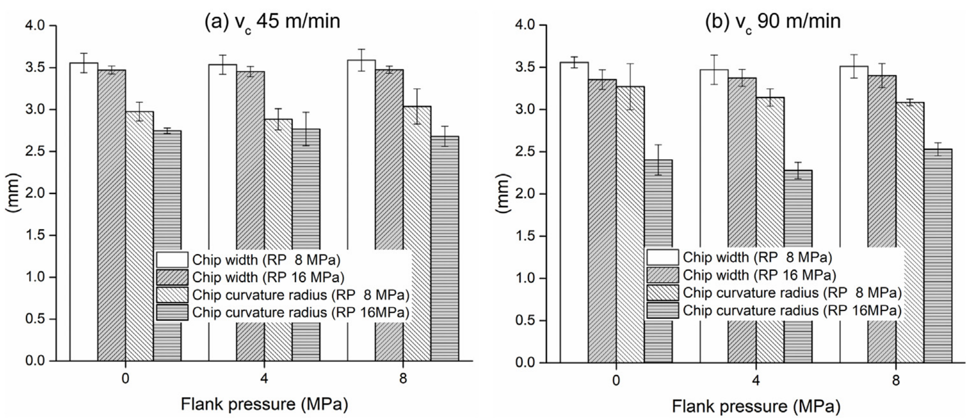

Fig. 9. Comparison of the chip width and chip curvature radius for different rake pressures, flank pressures and two cutting speeds.

studied and documented with respect to the combined influence from the applied media streams.

Summary of the findings:

- An increase in the rake pressure from 8 to 16 MPa contributes to a significant reduction of the apparent TCC_{area} at both cutting speeds (45 and 90 m/min). Even though at a lower degree for the higher cutting speed. The reduction of the TCC_{area} ranges from 13 to 28 pct. see Fig. 7(a and b).
- The flank pressure contributes to the reduction of the TCC_{area} which is improved for both the tested rake pressures (4 and 8 MPa). It can be noted that at the lower cutting speed (45 m/min), the combined effect of cutting fluid supplied at 8 MPa to both the rake and the flank side of the insert creates almost the same reduction in TCC_{area} as a single coolant jet supplied at 16 MPa directed to the rake side of the insert only.
- Having additional cutting fluid on the flank face obviously leads to improved heat flux in the cutting zone leading to cooler chips and better chip breakability.
- There was only a small improvement (reduction) in TCC_{area} by an increase of the flank pressure from 0 and 4 MPa.
- At the higher cutting speed (90 m/min), the increase of flank pressure has a less pronounced effect on the control of the TCC_{area}.

The results and influence of high-pressure cooling in the present study can be correlated to different researcher's findings, such as:

Shaw [29] described during machining nickel, the maximum temperature is focussed on the cutting edge. Having the cutting fluid applied to the flank face can lower the tool wear and peak cutting temperature. In our findings, we could also see that having flank cooling has quantitively confirmed the influence of cutting fluid on TCC_{area} at lower cutting speed.

Further, Courbon et al. [30] found that an increase in nozzle diameter and pressure, as well as an impact point close to the cutting edge, influences the tool-chip contact length. This leads to reduced cutting forces and improved tool life. Significant results were observed at low cutting speeds. Our experiments were planned with constant nozzles diameter but an increase in rake pressure. The results emphasise again increases in pressure decreased the TCC_{area} by 13–28 pct.

da Silva et al. [31], referenced to the works of Trent and Wright [32], that the cutting fluid cannot access the seizure zone due to the strong atomic bonds and contact between the members of the tool-chip interface. However, an increase in the cutting fluid pressure may lead to media penetrating through the sliding zone lowering the contact area, friction and heat generated. Machado and Wallbank [33], results of machining of titanium alloy with high-pressure cutting fluid reduced the sticking and sliding zones up to 30 pct. as compared to a conventional flood cooling system. Our quantitative measurement of the TCC_{area} which indicates a proportional area reduction coupled with the increase in rake pressure aligns well with findings of da Silva et al. as well as Machado and Wallbank. However, we would like to point out that by having flank cooling, an advantage for improved heat flux is created despite the limited cutting fluid access to the cutting contact zone.

It was observed in the present study that for all the investigated cutting conditions, the experiments at 16 MPa of rake pressure had a significant effect over the 8 MPa rake pressure in lowering the tool-chip contact area.

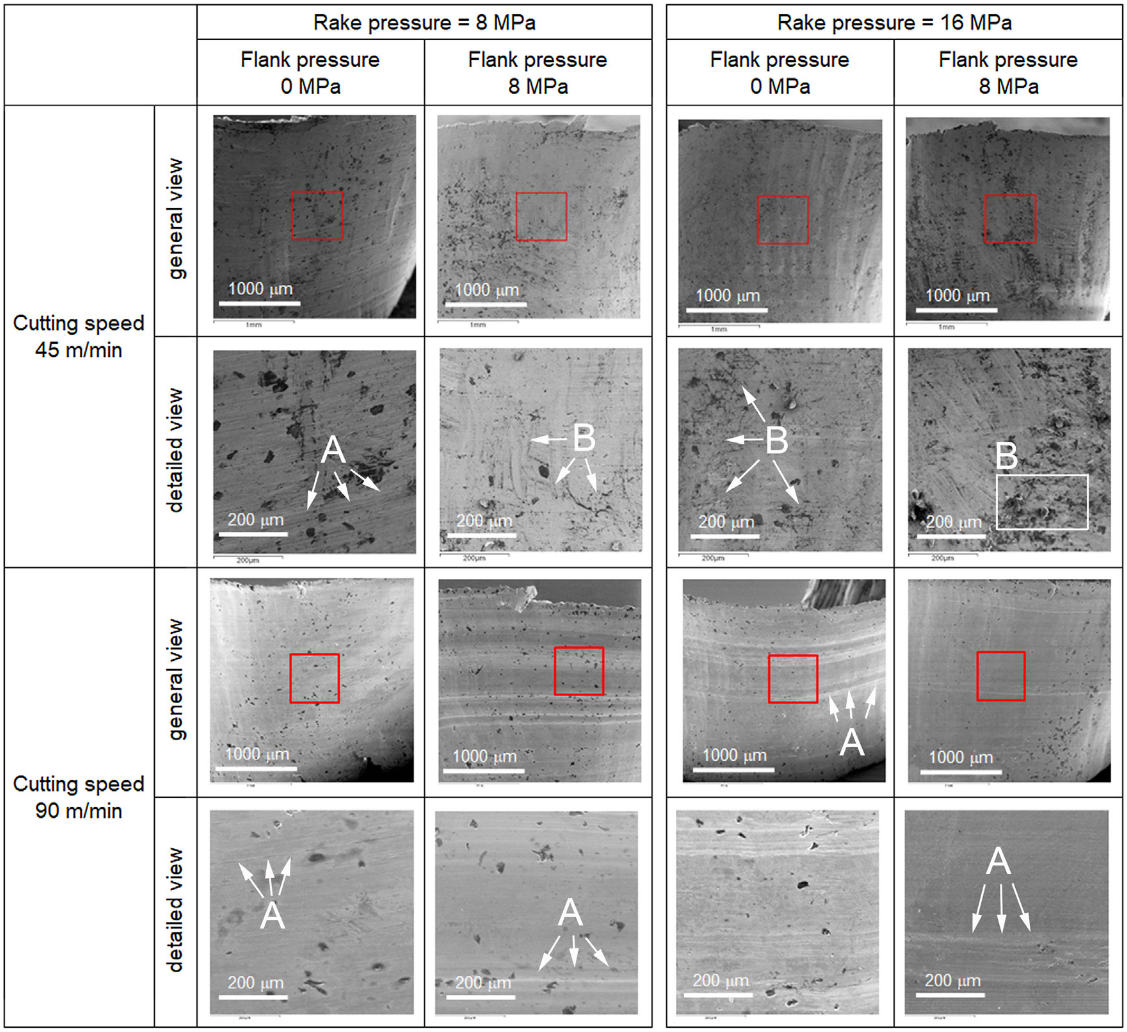

Fig. 10. SE micrographs of chips in general and detailed view (marked on the general view) — comparison of chip tool side for two rake pressures, flank pressures and cutting speeds.

Chip investigation

A chip investigation is a fundamental approach to the study of phenomena during a machining (chip formation) process. The chip reflects all the important facets of the cutting process. Thus, the chip is usually studied in detail when selected process parameters are evaluated towards process robustness. However, frequently only a limited subset of chip parameters are evaluated [32]. Therefore, in this particular investigation, a wide spectrum of chip parameters was investigated in relation to the flank pressure cooling concept, in order to obtain a detailed understanding of its impact on the cutting process.

Thus, the investigation of the chip formation process was done to understand the effect of the rake and flank pressure cooling at various cutting speeds. The chips were collected after each experiment and then evaluated individually, and the study of the chips was done in a few successive steps:

- First, the chip breakability, curvature radius and chip width were investigated.
- Next, chip morphology and chip tool side were explored.
- Finally, metallographic processing was performed.

The responses can be found summarized in Table 2.

Chip breakability, curvature radius and width

The shape, length and curvature radius of the chip was inspected first. The most typical representatives of chips were selected at each condition for evaluation.

The spiral shape of the chip was monitored and described for all cutting and cooling conditions. Nevertheless, the chip had various lengths, see Fig. 8. Chip breakability observations are aligned to the previous researchers' findings; that an increase in pressure leads to smaller (shorter) chips, regardless of the tool geometry, process or cutting conditions. It also showed that smaller chips were dominant at the speed of 90 m/min.

Additional flank pressure had an impact on the chip length, especially at lower rake pressure (8 MPa). A higher flank pressure (8 MPa) improved chip breakability (smaller chips) compared to no flank cooling, highlighted in Fig. 8. As stated earlier additional cooling led to improved heat flux in the cutting zone. Hence creating a cooler cutting interface that led to better chip breakability compared to no flank cooling.

This phenomenon was also present at a higher cutting speed with a less significant effect. Thus, when a very high media pressure towards the rake is not available, additional flank pressure up to 8 MPa can support the control of the chip formation process. The same effect of flank pressure was also observed for 16 MPa directed towards the rake at a speed of 45 m/min. However,

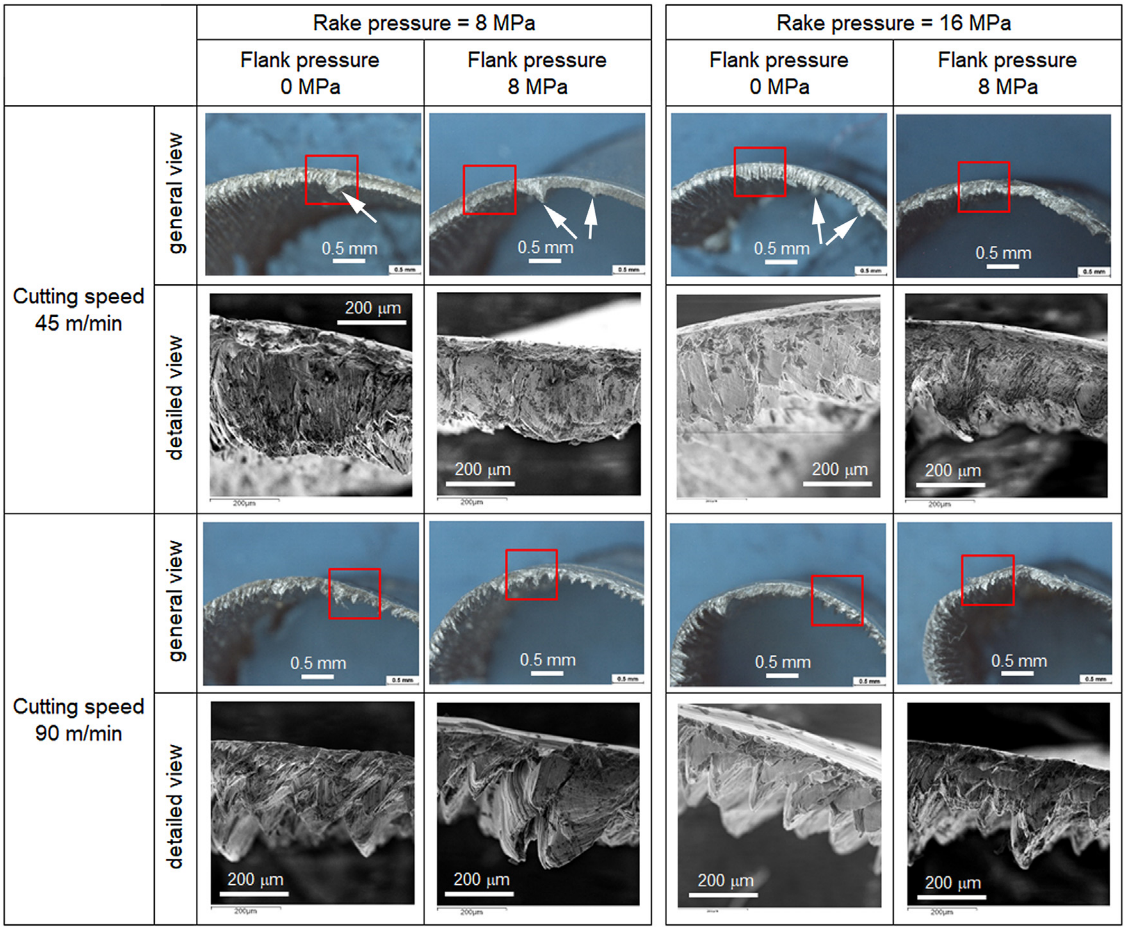

Fig. 11. Comparison of the chips at different rake pressures, flank pressures and cutting speeds: evaluation general view (LOM) and detailed view (SEM-SE).

the high pressure towards the rake dominantly influenced the chip length.

The following steps were followed during the chip analysis. Ten chips from each combination of cooling condition and cutting speed (v_c) were chosen, with the intention to inspect the chip width and chip curvature (chip radius). It was found that:

- The chip width was very stable during the whole experiment as can be seen in Fig. 9. However, a slight drop of the width with increasing rake pressure can be recognized because the chip is more deformed and curved in the direction orthogonal to the feed motion.
- The deformation of the chip at the higher cutting fluid pressures can be a result of a higher thermal gradient between the tool and the free side of the chip, but also from a higher cooling rate of the heated chip. Nevertheless, no significant influence of v_c and flank pressures on chip width was observed.

The chip curvature (the chip spiral radius) showed similar behaviour as the chip width, see Fig. 9. However, the change of the chip curvature (chip deformation in the direction of the chip flow) is more significant, especially at 90 m/min (the chip is likely hotter).

The smaller diameter of the chip at the higher cutting speed is a result of the acting fluid flow from rake cooling on thinner chip and probably its higher thermal gradient along the chip thickness. Thus, the chip tends to be more curved and breaks into smaller parts depending on the cutting speed as well as the increase in rake pressure owing to a hydro-dynamic wedge lifting the chip off rake face, e.g. [4,10]. Variation of cutting fluid pressure applied to the flank has almost no influence on this parameter. Since there is no direct effect as cooling and hydro-wedge on the chip as the rake face. This applies to both cutting speeds. However, the chip spirals (the chips) are typically shorter at lower rake pressure (Fig. 8) while the chip width and curvature radius are almost the same (Fig. 9). One of the reasons for this behaviour can be a lower temperature in the primary shear zone due to the additional flow of cutting fluid jet on the flank face resulting in higher brittleness of the chip.

Chip tool-side surface and segmentation

The tool side of the chips (*backside*) were inspected with SEM, see Fig. 10(i) general view and (ii) detailed view. Two elementary phenomena, sliding and sticking contact between the tool rake and the chip, were observed and found to be dependent on the cooling and cutting conditions.

The sliding is expected when the temperature of the chip in the secondary shear zone is high and the material is softer. In these conditions, higher cutting speed and/or insufficient cooling of the zone is set — e.g., when rake pressure is not high enough to penetrate deeply into the tool-chip interface to cool down the region effectively. Thus, the abrasion marks created by the tool in the direction of chip flow can be identified — arrows (A) in Fig. 10.

Intensive sticking contact was observed in the tool-chip contact zone at the lower cutting speed. Thus, the evident sticking marks. The regions of adhesion (sticking) were identified for some conditions – marks are identified by arrows (B); region (B) in Fig. 10. This is in accordance with Refs. [34,35] where the length of

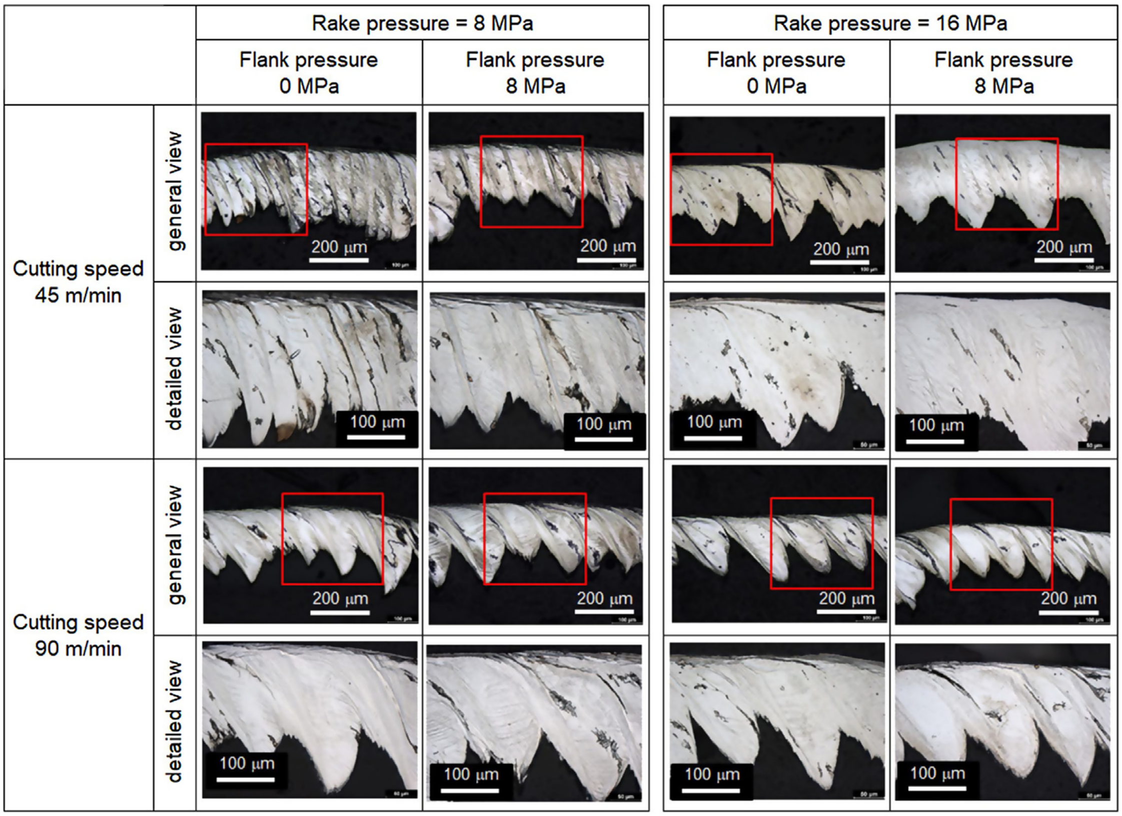

Fig. 12. SE micrographs for comparison of the chip structure for different rake pressures, flank pressures and the two cutting speeds.

Table 3
Results of chip characterization measurement.

Cutting speed v_c (m/min)	Rake pressure RP (MPa)	Flank pressure FP (MPa)	Segment orientation angle Φ (°)	Min chip thickness t_{min} (μm)	Max chip thickness t_{max} (μm)	Chip ratio t_{max}/t_{min}	Segment width S (μm)	Eq. chip thickness t_c (μm)	Segment ratio G_s	Shear angle ϕ (°)	Shrinkage factor ζ
45	8	0	13.3	213	261	1.22	51	237	0.18	10.2	0.19
		8	13.6	195	276	1.42	77	235	0.29	9.8	0.18
	16	0	25.5	151	235	1.55	88	193	0.35	21.6	0.42
		8	20.4	184	241	1.31	150	212	0.24	16.8	0.32
90	8	0	30.9	143	228	1.60	79	185	0.37	26.8	0.55
		8	29.4	150	249	1.65	120	199	0.40	23.3	0.46
	16	0	38.0	87	202	2.32	116	145	0.57	37.4	0.87
		8	33.1	108	203	1.88	106	155	0.47	32.7	0.71

the sticking region was measured and found to be lower and possible to predict with higher speed. And at higher rake pressure of cutting fluid, the tool-chip contact length decreases as shown in Ref. [36]. Thus, the length of the sliding region is shorter [5] in the case of higher cutting fluid pressure and low cutting speed. Thus, material softening of the chip is not as significant owing to: (i) enough pressure and volume of cutting fluid; (ii) lower cutting speed; (iii) combination of both.

Results from the lower cutting speed (45 m/min) illustrate that the rake pressure can affect the contact conditions between the chip and tool rake. These changes in the sliding zone of the contact were observed utilizing the tool-side of the chip inspection. More abrasion marks indicate more severe sliding conditions at 8 MPa or a shorter sliding region length in the case of 16 MPa, respectively. It aligns with the fact that at high rake pressure, the cutting fluid can penetrate deeply into the tool-chip interface and thereby reduce the sliding region [10,11].

The use of flank cooling on the tool probably further assisted in lowering the temperature in the cutting zone. This is the result of an increase in the cutting fluid volumetric flow, as reported in Ref. [7]. Subsequently influencing the temperature in the cutting zone and tool-chip interface is affected indirectly because of the intensive sticking behaviour between the tool and the chip. It was clear that more sticking marks on the chips were observed at a flank pressure of 8 MPa for both rake pressures (at 45 m/min).

Increasing the cutting speed to 90 m/min had a dominant effect on sliding in the secondary shear zone, arrows (A) Fig. 10. The changes in cutting fluid pressures (flank pressure and higher rake pressure) did not affect the sliding much. Therefore, a higher rake pressure than 16 MPa is recommended for cooling the tool-chip interface at this speed.

The chips were scanned from the side of the maximum chip thickness (see Fig. 5(c)). The main results at low/high magnification from two flank pressure conditions (0 and 8 MPa) are shown in

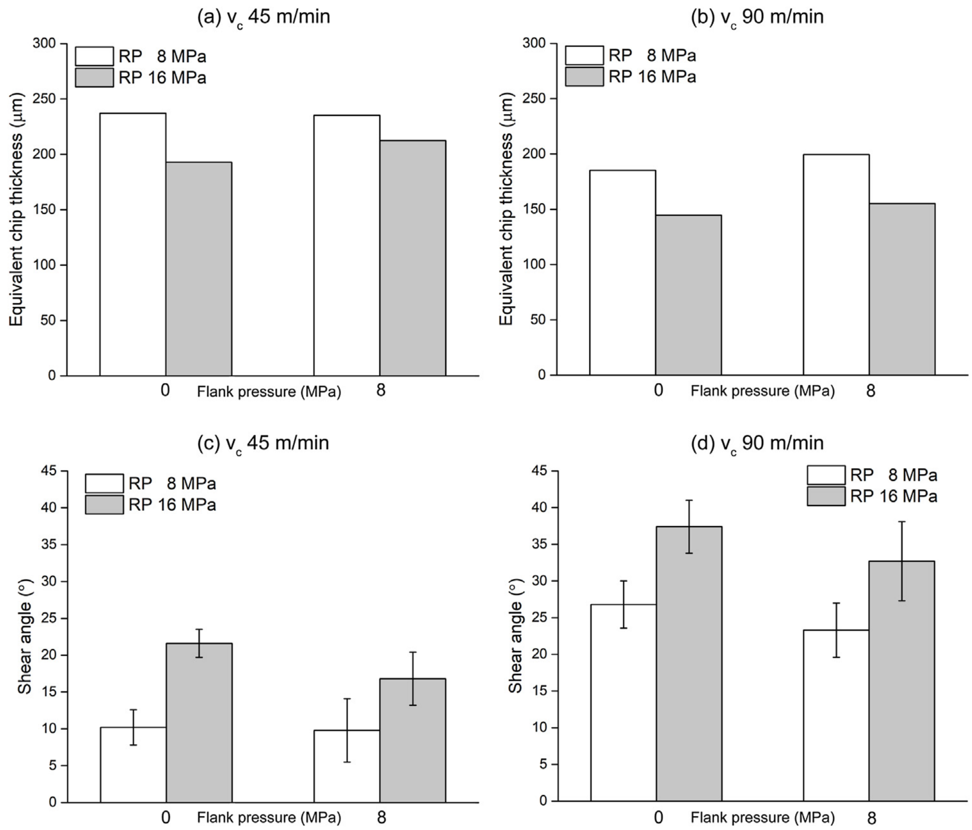

Fig. 13. For different rake and flank pressures: Equivalent chip thickness (a) low v_c (b) high v_c; Shear angle (c) low v_c (d) high v_c.

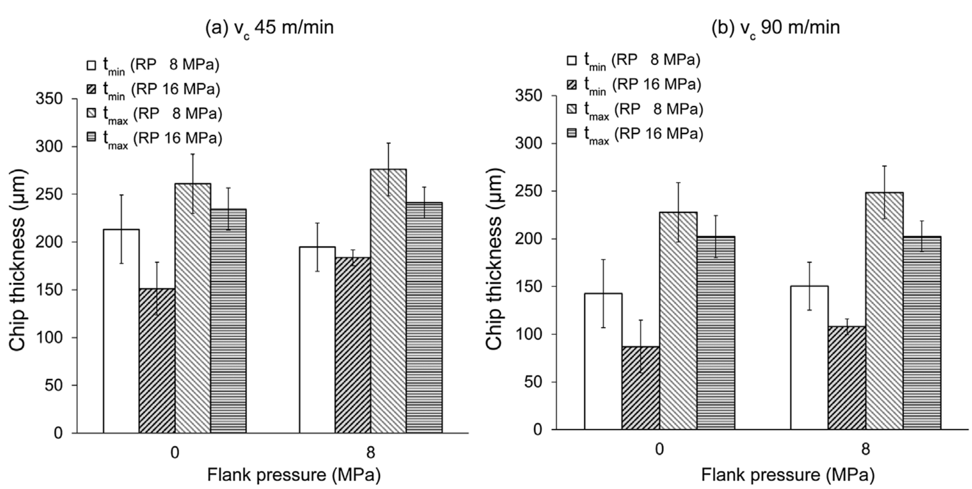

Fig. 14. Comparison of t_{min} and t_{max} between different rake pressures, flank pressures and cutting speeds.

Fig. 11. The general (LOM) and the selected area (highlighted in a red square in general view) are visualized in a detailed (SEM) view. The uniformity of the chip creation along the longer chip flow was observed. It is obvious that there could occur some parts of chips with anomalies in the shape and formation, *as marked by arrows*. These parts were excluded for the metallographic evaluation of the chips. The anomalies were found in chips especially generated at cutting speed of 45 m/min. The chip segmentation was more uniform (the anomalies were reduced) with higher chip segmentation at higher speed and higher rake pressure of coolant.

Metallographic processing of chips and calculations

The metallographic evaluation of the chips was conducted in order to understand the chip segmentation phenomenon better. Chip structure after polishing and etching for various cooling conditions and v_c can be observed in Fig. 12.

Continuous chips were generated at the lower cutting speed, v_c 45 m/min and rake pressure (8 MPa). However, shear localisation was not evident as a large volume of material underwent deformation. However, shear localisation in the chips was observed for the same rake pressure but at the increased cutting

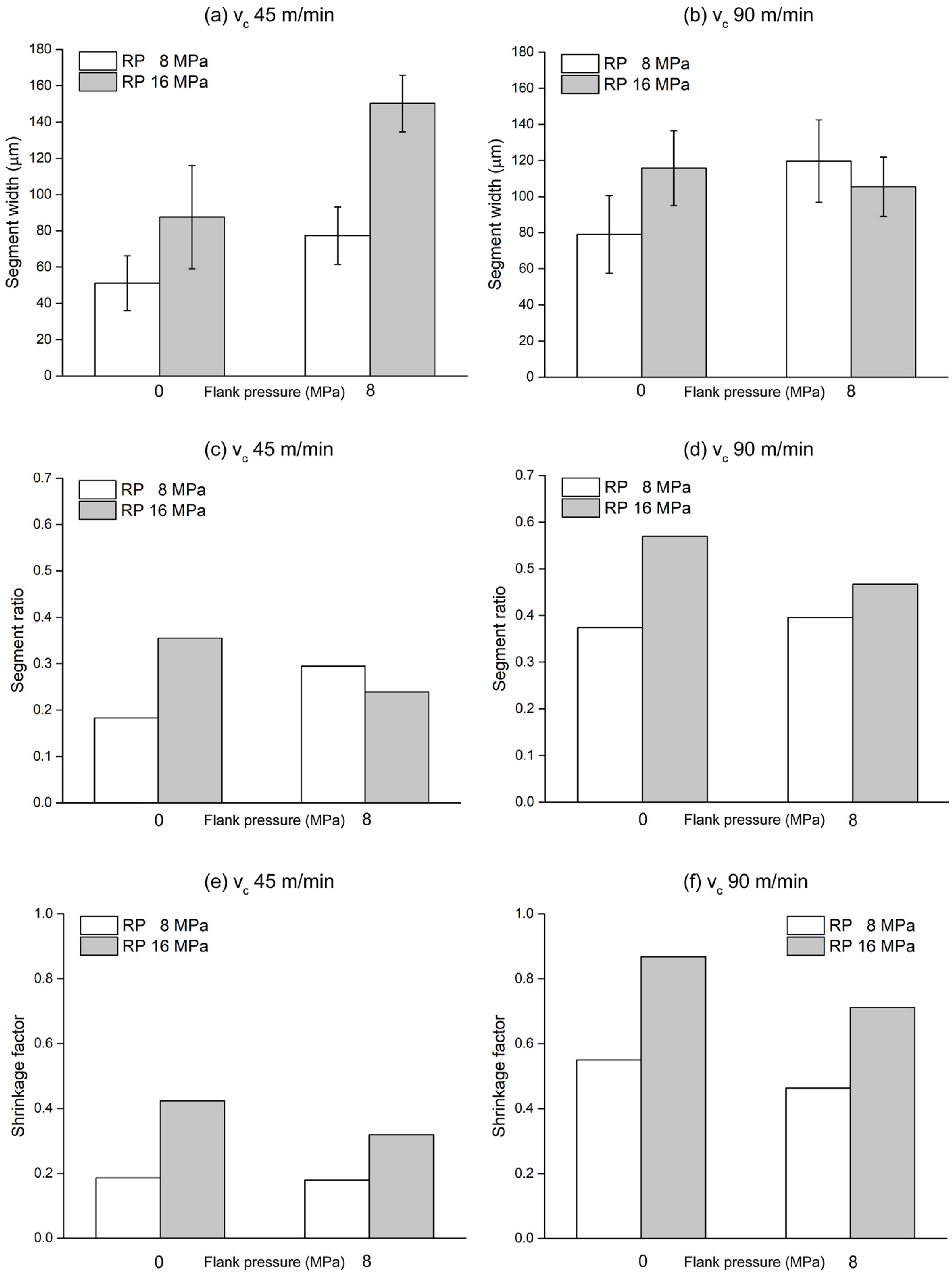

Fig. 15. For different rake and flank pressures: segment width (a) low v_c (b) high v_c; segment ratio (c) low v_c (d) high v_c; shrinkage factor (e) low v_c (f) high v_c.

speed, v_c 90 m/min. All the chips were serrated regardless of the cutting fluid conditions. It is evident that the chip segments get a shape that is increasingly uniform and regular with increased cutting speed.

Thakur et al. [37], conducted a high-speed dry turning machinability test of Alloy 718 with cemented carbide inserts. Although the experiment was *dry machining*, the findings of chip formation/morphology could support the current research work. The authors found that at higher cutting speeds than 50 m/min the cutting temperature was increased, due to the low thermal conductivity of the Alloy 718. This caused the chips to be more serrated than at lower cutting speeds. It is in accordance with the theory that shear instability occurs at a higher cutting speed (strain rate).

The effect of higher rake pressure (16 MPa) was similar to increased v_c. The chips were more serrated and uniform in shape. Using higher rake pressure for lower cutting speed leads to the initiation of the serration process of the chip, *marked in box* Fig. 12.

Table 4
Summary of chip characteristics as function of flank pressure increase from 0 to 8 MPa for rake pressure and cutting speed (m/min).

S.no	Chip characteristic	RP = 8 MPa		RP = 16 MPa	
		45 m/min	90 m/min	45 m/min	90 m/min
1	Chip width	⇔ +0.99	⇔ −1.29	⇔ +0.11	⇔ +1.43
2	Chip curvature radius	⇔ +2.09	⇓ −5.68	⇔ −2.46	⇑ +5.25
3	Maximum chip thickness	⇑ +5.7	⇑ +9.1	⇔ +2.9	⇔ +0.1
4	Minimum chip thickness	⇓ −8.8	⇑ +5.4	⇑ +21.4	⇑ +23.9
5	Equivalent chip thickness	⇔ −0.8	⇑ +7.6	⇑ +9.8	⇑ +6.9
6	Segment width	⇑ +51.1	⇑ +51.4	⇑ +71.6	⇓ −8.8
7	Shrinkage factor	⇔ −5.3	⇓ −16.4	⇓ −23.8	⇓ −18.4
8	Segment ratio	⇑ +61.1	⇑ +8.1	⇓ −31.4	⇓ −17.5
9	Shear angle	⇔ −3.7	⇓ −13.2	⇓ −22.1	⇓ −12.8

It can be identified as a transition region between continuous and fully serrated chips. Rake pressure supported chip segmentation by means of higher shear localisation. The transition region of chip formation from continuous to “serrated” was obtained by using the higher rake pressure.

The higher flank pressure (8 MPa) did not have any considerable influence on shear localisation, although, chip thickness started to vary. Specifically, the segments were bigger with flank cooling for both rake pressures at 45 m/min. Further, the chip morphology was more “serrated” and a slight influence on the chip segmentation could be seen for both rake pressures at the higher v_c 90 m/min. However, with flank cooling, the chips appeared to transition towards a more serrated shape, especially at a rake pressure of 8 MPa.

Eventually, chip morphology parameters were defined and used for an objective understanding of the chip formation and shear localisation. Results from all evaluated/calculated parameters of the chips are shown in Table 3.

It is a known behaviour that an increase in cutting speed leads to a higher shear angle [38,39] which was validated by our observation for an oblique cutting application, Fig. 13(c–d).

The effect of a higher strain rate on work material softening and resulting flow stress in the primary shear zone causes the inclination of the zone towards the tool rake and the chip becomes thinner. This result aligns with other researchers findings as reported in Refs. [40–42]. Consequently, a higher shear angle occurs with increased cutting speed. This behaviour was observed for all investigated cooling conditions [43].

Even though rake pressure does not influence the primary shear zone but influences chip formation and chip sliding on the tool. Thus, the chips are thinner (equivalent chip thickness — t_c) and more curved (proved for every chip thickness parameter as well as for chip curvature at all combinations of v_c and flank pressures).

A slight drop of the shear angle was identified at flank pressure 8 MPa. This indicates that flank cooling can influence phenomena taking place in the primary shear zone like the temperature of the deformed material.

Minimum and maximum segment thickness decreases significantly with cutting speed for all cooling conditions, see Fig. 14(a–b). The segments are more separated from each other since the equivalent chip thickness is decreasing as well, Fig. 13(a–b).

Higher rake pressure leads to a decrease of maximum, minimum and equivalent thicknesses of the chips. On the contrary, flank pressure does not influence the chip thickness and segments separation markedly.

The width of the chip segments is strongly influenced by whether the chip is fully serrated (90 m/min), continuous or semi-serrated (transition between continuous and serrated chips at 45 m/min), Fig. 15(a–b). The parameter S was increasing with speed as the shear zone becomes narrower owing to thermo-mechanical instability and thermal softening of the material. In general, similar behaviour in segment pitch with cutting speed for turning Inconel 718 was observed in Refs. [42,44], however it was under dry conditions.

It was observed that the segments were wider with increasing rake pressure at 45 m/min disregarding the flank cooling condition. The same effect of rake cutting fluid pressure was determined in Ref. [13]. The presence of flank cooling improved the chip segmentation (see Fig. 12). Thus, rake and flank cutting fluid at high pressures support shear instability and serrated chip formation owing to changed friction conditions on both interfaces; tool-chip and tool-machined surface. The result of a higher shear angle with increased rake pressure affects chip serration. Although as previously reported, flank pressure decreases the shear angle. The observed effect reached its limit when already fully serrated chips were generated at 90 m/min. On one hand, the segment width increased during flank cooling at 8 MPa and a rake pressure of 8 MPa, on the other hand, flank cooling led to a slightly lower width of the chip segments at a rake pressure of 16 MPa. This could indicate that no simple effect of flank pressure exists for serrated chips and high-pressure cutting fluid on the rake face.

A higher value of segment ratio means that the segments are more separated from each other i.e., better chip breakability is expected. This parameter increased with cutting speed, see Fig. 15(c–d). Similar results were shown in the study Sánchez Hernández et al. [18] for turning titanium alloy at lower feeds. The same phenomenon was determined under dry conditions in turning Inconel 718 in Klocke et al. [45].

A similar influence was observed with the rake pressure for both speeds when no flank cutting fluid was used. The higher pressure of cutting fluid brought the above-mentioned phenomena supporting chip segmentation. The hydro-dynamic wedge of cutting fluid helps the segment movement in the direction of the shear plane. Higher rake pressure caused a higher separation of segments. The characteristics t_{cmax} and t_{cmin} were decreasing with pressure for both speeds these results are in accordance with the findings of Cayli [46]. Although the more progressive decrease of t_{cmax} caused decreasing of G_s there. The difference between both results can be caused by different work materials as well as another machining operation and cooling conditions.

It was proved at both cutting speeds that flank cutting fluid at 8 MPa increased the segment ratio at a rake pressure of 8 MPa but decreased the ratio for a rake pressure of 16 MPa. This is in correlation with t_{cmin} and t_{cmax} changes. For both speeds, t_{cmin} was lower when flank pressure was applied together with rake pressure of 8 MPa. On the other hand, it increased with the rake pressure of 16 MPa. Nevertheless, the effect of flank pressure on t_{cmax} was recognized as almost negligible. Although the segments were less separated from each other, chip breakability was not influenced. This correlates with our previous observation that flank pressure supports chip segmentation and breakability when not enough rake pressure is used. As was already shown, flank pressure lowers the shear angle as well as supports shear instability under conditions at the start of the serrated chip creation region. When the chip is already highly serrated, the flank pressure effect causes decreasing G_s owing to t_{cmin} increasing as the shear angle is significantly lower.

Values of the shrinkage factor are illustrated in Fig. 15(e–f). Higher values of the factor were achieved at high v_c since the shear angle was higher. Sánchez Hernández et al. [18] observed for dry turning of titanium rather different results strongly dependent on feed. However, the behaviour was similar at lower feeds. Contrary to this, are the results in Pawade and Joshi [42]. In the high-speed dry turning of Inconel 718 was the ratio of t_{cmin} and t_{cmax} progressively decreasing with cutting speed due to an increase of chip thickness. Nevertheless, Rakesh and Datta [44] showed a decrease in chip thickness for dry turning of the same material for speed in the range from 50 to 75 m/min.

The results show that rake cutting fluid influenced chip thickness as well as the shrinkage factor. A similar effect was observed with an increase in rake pressure (as in Refs. [13,14,47,48]), which was following the shear angle behaviour. However, most importantly flank cooling (8 MPa) decreased the factor for both v_c and rake pressures. An immense increase in the chip shrinkage (approx. two-fold) was visible at increased v_c.

The effects of the flank pressure (an increase from 0 to 8 MPa) for all the combinations of two rake pressures and two cutting speeds are summarized in Table 4. Every value was expressed as a percentage change of the nominal value. The nominal values were for each parameter with reference to no flank cooling. Arrows indicate if the parameter increased, decreased, or stayed constant. The interval for no significant change of the value was set as −3 to +3%.

Conclusion

- **Tool-chip contact area**: Increase in rake pressure from 8 to 16 MPa, certainly decreased the mean contact area by 13–28% for all flank pressure conditions at both v_c. m/min. At low v_c, 8 MPa flank cooling lowered the contact area, on the contrary, at high v_c flank cooling did not have any significant effect.
- **Chip geometry:**
  - Chip width and chip curvature radius are lower with an increase in rake pressure as the hydro-wedge effect lifting the chip off the rake face. It results in shorter contact length and higher heat dissipation owing to an increased volumetric flow of cutting fluid.
  - At lower cutting speed the chips were shorter (increased breakability) with flank pressure cooling.
- **Chip texture:**
  - Higher rake pressure (16 MPa) showed more indication of sticking marks on chips because of the sliding region reduction, especially at lower v_c.
  - Lower rake pressure (8 MPa), additional flank cooling of 8 MPa leads to increase sticking in the tool-chip interface. This supports the indirect observation that flank pressure could have helped to lower the temperature in the cutting zone. Almost no adhesion on the chip was observed at a higher cutting speed. Thus, the sliding zone was not influenced significantly.
- **Chip formation:**
  - A thinner chip was generated when the cutting speed changed from 45 to 90 m/min as the shear angle increased.
  - Adding flank cooling decreased the shear plan angle at low and high cutting speeds.
- **Chip segmentation:**
  - Flank cooling (8 MPa) supports the chip segmentation process.
  - Flank pressure can affect the chip formation process by temperature reduction in the shear zone. It facilitates embrittlement of the chip and enhanced shear work. Subsequently, better chip breaking occurs.

Conflicts of interest

The authors declare no conflict of interest. The funding agencies had no role in the experiments, analysis, or interpretation of data and in the decision to publish the results.

Acknowledgements

The authors would like to thank both the national funding organizations/projects, Sweden: Västra Götalands Regionen (VGR), PROSAM project (Dnr RUN 612-0974-13) and Czech Republic: This work was supported by the project Novel nanostructures for engineering applications No. CZ.02.1.01/0.0/0.016 026/0008396. We would also like to thank Sandvik Coromant for the support with inserts. A special thanks goes to Andreas Gustafsson at University West and Andreas Lindberg at GKN Aerospace Engine Systems AB for helping with experiments. Saurck Clemens, Bruker Alicona, Austria in helping with the license of 3-D measurement software.

References

[1] Tamil Alagan, N., Hoier, P., Zeman, P., Klement, U., Beno, T., Wretland, A., 2019, Effects of High-Pressure Cooling in the Flank and Rake Faces of WC Tool on the Tool Wear Mechanism and Process Conditions in Turning of Alloy 718. Wear, 434–435/September: 102922. http://dx.doi.org/10.1016/j.wear.2019.05.037.
[2] Klocke, F., Sangermann, H., Krämer, A., Lung, D., 2011, Influence of a High-Pressure Lubricoolant Supply on Thermo-Mechanical Tool Load and Tool Wear Behaviour in the Turning of Aerospace Materials. Proceedings of the Institution of Mechanical Engineers Part B: Journal of Engineering Manufacture, 225/January (1): 1. http://dx.doi.org/10.1177/09544054JEM2082.
[3] Armarego, E.J.A., Brown, R.H., 1969, The Machining of Metals. Prentice-Hall.
[4] Sharman, A.R.C., Hughes, J.I., Ridgway, K., 2008, Surface Integrity and Tool Life when Turning Inconel 718 Using Ultra-High Pressure and Flood Coolant Systems. Proceedings of the Institution of Mechanical Engineers Part B: Journal of Engineering Manufacture, 222/June (6): 6. http://dx.doi.org/10.1243/09544054JEM936.
[5] Machado, A.R., Wallbank, J., 1994, The Effect of a High-Pressure Jet on Machining. Proceedings of the Institution of Mechanical Engineers, 208.
[6] Seid Ahmed, Y., Paiva, J.M., Veldhuis, S.C., 2019, Characterization and Prediction of Chip Formation Dynamics in Machining Austenitic Stainless Steel through Supply of a High-Pressure Coolant. International Journal of Advanced Manufacturing Technology, 102/June (5): 5. http://dx.doi.org/10.1007/s00170-018-03277-7.
[7] Dahlman, P., 2002, A Comparison of Temperature Reduction in High-Pressure Jet-Assisted Turning Using High Pressure Versus High Flowrate. Proceedings of the Institution of Mechanical Engineers Part B: Journal of Engineering Manufacture, 216/April (4): 4. http://dx.doi.org/10.1243/0954405021520067.
[8] Klocke, F., Cayli, T., Veselovac, D., 2016, Increasing Productivity and Process Stability in Turning of Aerospace Materials with High Pressure Lubricoolant Supply. Materials Science Forum, 836–837:48–55. http://dx.doi.org/10.4028/www.scientific.net/MSF.836-837.48.
[9] Jawahir, I.S., van Luttervelt, C.A., 1993, Recent Developments in Chip Control Research and Applications. CIRP Annals — Manufacturing Technology, 42/January (2): 2. http://dx.doi.org/10.1016/S0007-8506(07)62531-1.

[10] Ezugwu, E.O., Bonney, J., 2004, Effect of High-Pressure Coolant Supply when Machining Nickel-Base, Inconel 718, Alloy with Coated Carbide Tools. Journal of Materials Processing Technology, 153–154/November: 1045–1050. http://dx.doi.org/10.1016/j.jmatprotec.2004.04.329.
[11] Çolak, O., 2012, Investigation on Machining Performance of Inconel 718 Under High Pressure Cooling Conditions. Strojniski Vestnik Journal Journal of Mechanical Engineering, 58/11: 11. http://dx.doi.org/10.5545/sv-jme.2012.730.
[12] Crafoord, R., Kaminski, J., Lagerberg, S., Ljungkrona, O., Wretland, A., 1999, Chip Control in Tube Turning Using a High-Pressure Water Jet. Proceedings of the Institution of Mechanical Engineers Part B: Journal of Engineering Manufacture, 213/8: 8.
[13] Öjmertz, K.M.C., Oskarson, H.-B., 1999, Wear on SiC-Whiskers Reinforced Ceramic Inserts when Cutting Inconel with Waterjet Assistance. Tribology Transactions, 42/January (3): 471–478. http://dx.doi.org/10.1080/10402009908982243.
[14] Khan, M.A., Mia, M., Dhar, N.R., 2017, High-Pressure Coolant on Flank and Rake Surfaces of Tool in Turning of Ti–6Al–4V: Investigations on Forces, Temperature, and Chips. International Journal of Advanced Manufacturing Technology, 90/May (5): 1977–1991. http://dx.doi.org/10.1007/s00170-016-9511-6.
[15] Tamil Alagan, N., Hoier, P., Beno, T., Klement, U., Wretland, A., 2020, Coolant Boiling and Cavitation Wear — A New Tool Wear Mechanism on WC Tools in Machining Alloy 718 with High-Pressure Coolant. Wear, 452–453/July: 203284. http://dx.doi.org/10.1016/j.wear.2020.203284.
[16] Tamil Alagan, N., Zeman, P., Hoier, P., Beno, T., Klement, U., 2019, Investigation of Micro-Textured Cutting Tools Used for Face Turning of Alloy 718 with High-Pressure Cooling. Journal of Manufacturing Processes, 37/January: 606–616. http://dx.doi.org/10.1016/j.jmapro.2018.12.023.
[17] Tamil Alagan, N., Beno, T., Hoier, P., Klement, U., Wretland, A., 2018, Influence of Surface Features for Increased Heat Dissipation on Tool Wear. Materials, 11/April (5): 664. http://dx.doi.org/10.3390/ma11050664.
[18] Sánchez Hernández, Y., Trujillo Vilches, F.J., Bermudo Gamboa, C., Sevilla Hurtado, L., 2018, Experimental Parametric Relationships for Chip Geometry in Dry Machining of the Ti6Al4V Alloy. Materials, 11/July (7). http://dx.doi.org/10.3390/ma11071260.
[19] Sánchez, Y., Trujillo, F.J., Sevilla, L., Marcos, M., 2015, Study of the Influence of the Cutting Parameters on the Chip Geometry During Machining Alloy UNS A97075. Procedia Engineering, 132/January: 513–520. http://dx.doi.org/10.1016/j.proeng.2015.12.527.
[20] Li, L., Wu, M., Liu, X., Cheng, Y., Yu, Y., 2018, Experimental Study of the Wear Behavior of PCBN Inserts During Cutting of GH4169 Superalloys Under High-Pressure Cooling. International Journal of Advanced Manufacturing Technology, 95/March (5): 1941–1951. http://dx.doi.org/10.1007/s00170-017-1333-7.
[21] Behera, B.C., Alemayehu, H., Ghosh, S., Rao, P.V., 2017, A Comparative Study of Recent Lubri-Coolant Strategies for Turning of Ni-Based Superalloy. Journal of Manufacturing Processes, 30/December: 541–552. http://dx.doi.org/10.1016/j.jmapro.2017.10.027.
[22] Tamil Alagan, N., 2019, Enhanced Heat Transfer and Tool Wear in High-Pressure Coolant Assisted Turning of Alloy 718. Doctoral thesis.(Accessed 3 February 2020). [Online]. Available: University West, Trollhättan *http://urn.kb.se/resolve?urn=urn:nbn:se:hv:diva-14663*.
[23] Abukhshim, N.A., Mativenga, P.T., Sheikh, M.A., 2004, An Investigation of the Tool-Chip Contact Length and Wear in High-Speed Turning of EN19 Steel. Proceedings of the Institution of Mechanical Engineers Part B: Journal of Engineering Manufacture, 218/August (8): 889–903. http://dx.doi.org/10.1243/0954405041486064.
[24] Stephenson, David A., 2006, Metal Cutting Theory and Practice. CRC Taylor & Francis.
[25] Klocke, F., Lung, D., Cayli, T., Döbbeler, B., Sangermann, H., 2014, Evaluation of Energy Efficiency in Cutting Aerospace Materials with High-Pressure Cooling Lubricant Supply. International Journal of Precision Engineering and Manufacturing, 15/June (6): 6. http://dx.doi.org/10.1007/s12541-014-0454-2.
[26] Klocke, F., Döbbeler, B., Lakner, T., 2018, Influence of the Coolant Nozzle Orientation and Size on the Tool Temperature Under High-Pressure Coolant Supply Using an Analogy Test Bench. Production Engineering, 12/June (3): 3. http://dx.doi.org/10.1007/s11740-018-0823-2.
[27] Zhang, C., Lu, J., Zhang, F., Butt, S.I., 2017, Identification of a New Friction Model at Tool-Chip Interface in Dry Orthogonal Cutting. International Journal of Advanced Manufacturing Technology, 89/March (1): 921–932. http://dx.doi.org/10.1007/s00170-016-9149-4.
[28] Altintas, Y., 2012, Manufacturing Automation. 2nd ed. Cambridge University Press — M.U.A, United Kingdom.
[29] Shaw, M.C., 2005, Metal Cutting Principles. 2. ed. Oxford University Press, New York.
[30] Courbon, C., Kramar, D., Krajnik, P., Pusavec, F., Rech, J., Kopac, J., 2009, Investigation of Machining Performance in High-Pressure Jet Assisted Turning of Inconel 718: An Experimental Study. International Journal of Machine Tools and Manufacture, 49/November: 1114–1125. http://dx.doi.org/10.1016/j.ijmachtools.2009.07.010.
[31] da Silva, R.B., Machado, Á.R., Ezugwu, E.O., Bonney, J., Sales, W.F., 2013, Tool Life and Wear Mechanisms in High Speed Machining of Ti–6Al–4V Alloy with PCD Tools Under Various Coolant Pressures. Journal of Materials Processing Technology, 213/August (8): 1459–1464. http://dx.doi.org/10.1016/j.jmatprotec.2013.03.008.
[32] Trent, E.M., Wright, P.K., 2000, Metal Cutting: Fourth Edition. 4th ed. Butterworth Heinemann, United States.
[33] Machado, A.R., Wallbank, J., 1990, Machining of Titanium and its Alloys—A Review. Proceedings of the Institution of Mechanical Engineers Part B: Journal of Engineering Manufacture, 204/February (1): 53–60. http://dx.doi.org/10.1243/PIME_PROC_1990_204_047_02.
[34] Ozlu, E., Molinari, A., Budak, E., 2010, Two-Zone Analytical Contact Model Applied to Orthogonal Cutting. Machining Science and Technology, 14/November (3): 323–343. http://dx.doi.org/10.1080/10910344.2010.512794.
[35] Li, M., Xu, D., Cui, Z., Xie, Z., 2020, Research on the Sticking-Sliding Contact Ratio in High-Speed Cutting of Cupronickel B10. Journal of Mechanical Science and Technology, 34/March (3): 1275–1282. http://dx.doi.org/10.1007/s12206-020-0226-0.
[36] Nandy, A.K., Gowrishankar, M.C., Paul, S., 2009, Some Studies on High-Pressure Cooling in Turning of Ti–6Al–4V. International Journal of Machine Tools and Manufacture, 49/February (2): 2. http://dx.doi.org/10.1016/j.ijmachtools.2008.08.008.
[37] Thakur, D.G., Ramamoorthy, B., Vijayaraghavan, L., 2009, Study on the Machinability Characteristics of Superalloy Inconel 718 During High Speed Turning. Materials & Design, 30/May (5): 5. http://dx.doi.org/10.1016/j.matdes.2008.07.011.
[38] Warsi, S.S., et al, 2017, Development of Energy Consumption Map for Orthogonal Machining of Al 6061-T6 Alloy. Proceedings of the Institution of Mechanical Engineers Part B: Journal of Engineering Manufacture, ;(April). http://dx.doi.org/10.1177/0954405417703424.
[39] Hao, M., Xu, D., Feng, P., 2019, Numerical and Experimental Investigation of the Shear Angle in High-Speed Cutting of Al6061-T6. International Journal of Advanced Manufacturing Technology, 100/February (9): 3037–3044. http://dx.doi.org/10.1007/s00170-018-2842-8.
[40] Jaspers, S.P.F.C., Dautzenberg, J.H., 2002, Material Behaviour in Conditions Similar to Metal Cutting: Flow Stress in the Primary Shear Zone. Journal of Materials Processing Technology, 122/March (2): 322–330. http://dx.doi.org/10.1016/S0924-0136(01)01228-6.
[41] Jaspers, S.P.F.C., Dautzenberg, J.H., 2002, Material Behaviour in Metal Cutting: Strains, Strain Rates and Temperatures in Chip Formation. Journal of Materials Processing Technology, 121/February (1): 123–135. http://dx.doi.org/10.1016/S0924-0136(01)01227-4.
[42] Pawade, R.S., Joshi, S.S., 2011, Mechanism of Chip Formation in High-Speed Turning of Inconel 718. Machining Science and Technology, 15/April (1): 132–152. http://dx.doi.org/10.1080/10910344.2011.557974.
[43] Brown, C.A., 2001, Machining of Metals: Fundamentals. in Buschow KK.H.J.HJ, Cahn RR.W.W, Flemings MM.C.C, Ilschner BB., Kramer EE.J.J, Mahajan SS., Veyssière PP., (Eds.) Encyclopedia of Materials: Science and Technology. Elsevier, Oxford, pp. pp.4703–4708. http://dx.doi.org/10.1016/B0-08-043152-6/00820-2.
[44] Rakesh, M., Datta, S., 2020, Machining of Inconel 718 Using Coated WC Tool: Effects of Cutting Speed on Chip Morphology and Mechanisms of Tool Wear. Arabian Journal for Science and Engineering, 45/February (2): 797–816. http://dx.doi.org/10.1007/s13369-019-04171-4.
[45] Klocke, F., Döbbeler, B., Peng, B., Schneider, S.A.M., 2018, Tool-Based Inverse Determination of Material Model of Direct Aged Alloy 718 for FEM Cutting Simulation. Procedia CIRP, 77/January: 54–57. http://dx.doi.org/10.1016/j.procir.2018.08.211.
[46] Cayli, T., 2018, Surface Anomalies in Turning of Difficult-to-Cut Materials with High-Pressure Coolant Supply.(Accessed 10 April 2021). [Online]. Available: Apprimus Wissenschaftsverlag, Aachen, Germany *http://ebookcentral.proquest.com/lib/vast-ebooks/detail.action?docID=5218507*.
[47] Thakur, A., Mohanty, A., Gangopadhyay, S., Maity, K.P., 2014, Tool Wear and Chip Characteristics during Dry Turning of Inconel 825. Procedia Materials Science, 5/January: 2169–2177. http://dx.doi.org/10.1016/j.mspro.2014.07.422.
[48] Parida, A.K., Maity, K., 2019, FEM Analysis and Experimental Investigation of Force and Chip Formation on Hot Turning of Inconel 625. Defence Technology, 15/December (6): 853–860. http://dx.doi.org/10.1016/j.dt.2019.04.012.